JOURNAL OF MATERIALS SCIENCE 32 (1997) 761–771

Shear ductility and toughenability study of highly cross-linked epoxy/polyethersulphone

H. KISHI*, Y-B. SHI, J. HUANG, A. F. YEE‡
Department of Materials Science and Engineering, University of Michigan, Dow Building, 2300 Hayward Street, Ann Arbor, Michigan 48109, USA

The objective of the present study was to determine whether the ductility and toughenability of a highly cross-linked epoxy resin, which has a high glass transition temperature, T_g, can be enhanced by the incorporation of a ductile thermoplastic resin. Diglycidyl ether of bisphenol-A (DGEBA) cured by diamino diphenyl sulphone (DDS) was used as the base resin. Polyethersulphone (PES) was used as the thermoplastic modifier. Fracture toughness and shear ductility tests were performed to characterize the materials. The fracture toughness of the DDS-cured epoxy was not enhanced by simply adding PES. However, in the presence of rubber particles as a third component, the toughness of the PES–rubber-modified epoxy was found to improve with increasing PES content. The toughening mechanisms were determined to be rubber cavitation, followed by plastic deformation of the matrix resin. It was also determined, through uniaxial compression tests, that the shear ductility of the DDS-cured epoxy was enhanced by the incorporation of PES. These results imply that the intrinsic ductility, which had been enhanced by the PES addition, was only activated under the stress state change due to the cavitation of the rubber particles. The availability of increasing matrix ductility seems to be responsible for the increase in toughness.

1. Introduction

Thermosetting resins, such as epoxy and phenolic resins, are widely used as structural materials and adhesives in the aerospace and electronics industries for their high strength, high elastic modulus, and good heat and solvent resistance. The good heat and solvent resistance have been reasoned to originate from their cross-linked chemical structure [1]. However, an undesirable result is their low fracture toughness relative to other families of polymer resins. Therefore, they need to be toughened in order to achieve an extended range of applications. It is known that relatively low cross-link epoxy resins can be toughened by the incorporation of elastomer particles, but more highly cross-linked epoxy resins are difficult to toughen in this way [2, 3].

Yee and co-workers [2, 4–6] have identified and elucidated the toughening mechanisms in the elastomer-toughening technique. According to these authors, the role of the elastomer particles is to relieve the constraint in front of the crack tip by cavitation [4, 5]. This mechanism then alters the stress field from one dominated by triaxial stress, which causes brittle fracture, to one dominated by shear stress [6], which promotes the formation of shear bands in the matrix resin [2, 4, 5]. The intrinsic ability of the matrix resin to deform plastically under high shear stress, i.e. the "shear ductility" of the matrix resin, is considered a vital requirement for the elastomer-toughening technique to be effective. This is because the actual amounts of shear deformation of the matrix resin around the cavitated particles should strongly depend on the ductility of the resin. Therefore, the lower elastomer-toughenability of highly cross-linked networks can be explained as a result of their low intrinsic ductility.

One simple way to increase the toughenability of thermosetting resins is to reduce the cross-link density. In many cases, however, reducing the cross-link density causes a decrease in the glass transition temperature, T_g, of the cured resin. To maintain a high T_g with reduced cross-link density, uncured resin monomers with a more rigid chemical backbone structure need to be used [7, 8]. However, epoxy monomers which have rigid chemical structures tend to be in a solid state at room temperature. This reduces their processability and limits their applicability. More research is therefore needed in order to overcome the trade-off between toughness, heat resistance and processability.

**Present address*: Toray Industries, Inc., Composite Materials Research Laboratories, 1515, Tsutsui, Masaki-cho, Iyogun, Ehime 791-31, Japan.
‡Author to whom all correspondence should be addressed.

0022–2461

Alternatively, Bucknall *et al.* [9] have attempted to enhance the toughenability of a highly cross-linked epoxy resin while keeping its highly cross-linked nature by incorporating a ductile thermoplastic resin. Unfortunately, they did not find an increase in the toughenability because of the decomposition of polycarbonate, which was used as the modifier, in the process. The concept that the toughenability of highly cross-linked resin can be enhanced by incorporating a ductile thermoplastic resin, however, is still attractive.

The objective of our current research was to determine whether the ductility and toughenability of a highly cross-linked epoxy resin can be enhanced by the incorporation of a ductile thermoplastic resin. A study is reported which shows that this concept is, indeed, valid by using polyethersulphone as the thermoplastic modifier.

2. Experimental procedure

2.1. Materials

The epoxy resin used in this investigation was DER332®, which consists of diglycidyl ethers of bisphenol-A (DGEBA), provided by the Dow Chemical Company. The epoxy equivalent weight of this resin is 174 $g\,eq^{-1}$. The resin was cured with the stoichiometric amount of 4,4′-diamino diphenyl sulphone (DDS), Sumicure-S®, provided by Sumitomo Chemical Co. The active amino-hydrogen equivalent weight of DDS is 62 $g\,eq^{-1}$. DDS-cured DER332 is known to be a highly cross-linked brittle epoxy, and carboxy-terminated butadiene–acrylonitrile liquid rubber (CTBN) modification is ineffective in toughening this epoxy [2]. Polyethersulphone (PES), Victrex 5003P® ($M_n = 23\,800\ g\,mol^{-1}$ [10]), which is an amorphous thermoplastic resin produced by ICI, was used as the modifier for increasing the ductility and toughenability of the DDS-cured epoxy resin. The chemical structures of these materials are shown in Fig. 1. Besides the DDS-cured DGEBA and the DDS-cured DGEBA/PES systems, a third system of DDS-cured DGEBA/PES modified with rubber was also studied in order to confirm whether the toughenability of DDS-cured epoxy could be enhanced by the incorporation of PES. Core–shell rubber particles, EXL2611®, produced by Rohm and Haas, were used for this purpose. The rubber particle has a polybutadiene core with a polymethylmethacrylate shell and has an average particle size of approximately 200 nm. One advantage of using pre-formed rubber particles over *in situ* formed particles based on liquid rubber, is that the composition and size of the particles can be controlled.

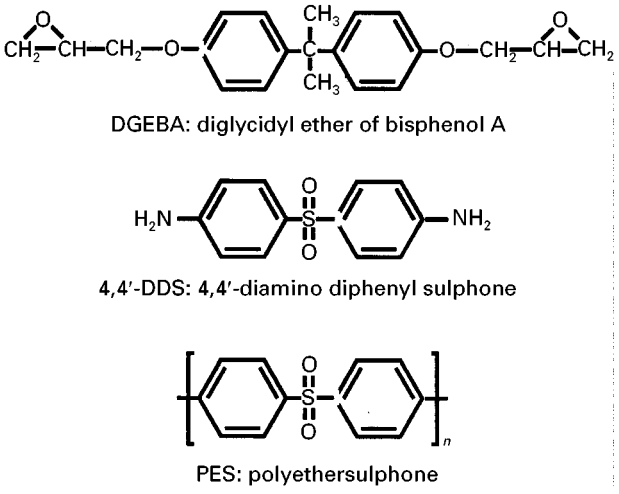

Figure 1 Chemical structures of the materials.

2.2. Preparation of blends

DDS-cured DGEBA/PES systems were prepared by the following procedure. First, PES powder was mixed with the epoxy resin at room temperature. To dissolve PES in the epoxy resin, the mixture was heated in an oil bath at 130 °C for 2 h. The mixture was stirred but care was taken to avoid mixing air into the liquid. After cooling the solution to under 80 °C, the stoichiometric amount of DDS was added to the resin, and the mixture was stirred for 30 min. The three-part mixture was then heated to 130 °C and was stirred for another 30 min in order to completely dissolve the DDS. This was followed by vacuum degassing for 15 min at the same temperature. Finally, the resin was cast into a pre-heated mould treated with a release agent. The mould was kept at 130 °C for 4 h, then heated up to 180 °C and kept for 2 h. After this curing procedure, the oven was switched off and the cured resin was allowed to cool slowly to room temperature.

The following procedure was used to prepare the DDS-cured DGEBA/rubber system. In order to disperse the rubber particles into the resin, methylethylketone (MEK) was used as a dispersing medium. First, the rubber particles were dispersed in MEK with ultrasonic wave vibration. Second, the DGEBA was slowly stirred into the rubber-dispersed MEK. Third, the resin mixture was heated at 100 °C for 3 h with stirring to remove most of the MEK and then was heated up to 130 °C under vacuum to remove the MEK completely. Finally after cooling the resin to 80 °C, the stoichiometric amount of DDS was added, and the resin was cured under the same procedures as described in the last paragraph.

In the case of preparing the DDS-cured DGEBA/PES/rubber ternary blend systems, the DGEBA had to be divided into two parts. One half was used to make rubber-dispersed epoxy, and the other half was used to make PES-dissolved epoxy. First, all the rubber particles were dispersed in MEK with ultrasonic wave vibration. Then, half of the DGEBA was stirred into the rubber-dispersed MEK. On the other hand, the PES powder was dissolved into the other half of the DGEBA by using the same conditions as mentioned previously. After evaporating most of the MEK from the DGEBA/rubber/MEK mixture with stirring at 100 °C, the PES-dissolved epoxy was poured into the rubber-dispersed epoxy at 100 °C. The mixture was subsequently stirred for 30 min. Then, the resin mixture was heated up to 130 °C under vacuum to remove the MEK completely. After cooling the resin to 80 °C, the stoichiometric amount of DDS was

added, and the resin was cured under the same procedure as in the previous two cases. This procedure was necessary because the rubber particles were difficult to disperse in a medium with high viscosity. If all the components were added at the same time, the PES would greatly increase the viscosity of the solution, and then dispersing the rubber would be nearly impossible.

2.3. Fracture toughness assessment

Fracture toughness of the DDS-cured DGEBA, DDS-cured DGEBA/PES systems, and several rubber-modified resins were measured in terms of the critical stress intensity factor, K_{IC}. K_{IC} values were determined using the single-edge notched three-point bending (SEN-3PB) method [11]. The dimensions of the specimens were 70 mm long $(L) \times 12.7$ mm wide $(W) \times 6.35$ mm thickness (B). The span for the bending test was 50.8 mm (S). The cracks were introduced by first cutting a notch using a low-speed diamond saw, then hammering in a razor blade which had been immersed in liquid nitrogen. Three-point bending tests were performed using a servo-hydraulic Instron testing machine (Model 1331) at a rate of 1 mm min^{-1}. At least six SEN-3PB specimens were tested for each system. The initial crack length, a, of each fractured specimen, needed for the calculation of K_{IC} values, was measured using an optical microscope. The initial crack length was within the range of 6.1 ± 0.5 mm to satisfy the geometry requirement. Linear elastic fracture mechanics was applied, and K_{IC} was calculated using the following relationships [12]

$$K_{IC} = Y\sigma_{max}a^{1/2} \quad (1)$$

$$\sigma_{max} = 3SF_{max}/(2BW^2) \quad (2)$$

where a is the initial crack length and F_{max} is the value of force at fracture. Y is a geometry factor, and for $S/W = 4$, which can be determined from Equation 3 [12]

$$Y = 1.93 - 3.07(a/W) + 14.53(a/W)^2 - 25.11(a/W)^3 + 25.80(a/W)^4 \quad (3)$$

2.4. Ductility assessment

2.4.1. Uniaxial compression test

It is known that the deformation and fracture behaviour of some materials depends strongly on the applied stress state. For example, even brittle polymers such as thermosetting resins, which do not yield under uniaxial tensile load, can exhibit ductile behaviour under uniaxial compression [1]. So, the ductility of the DDS-cured DGEBA and DDS-cured DGEBA/PES systems was assessed by using uniaxial compression tests in accordance with ASTM D695 [13]. The cylindrical specimens were 5 mm diameter and 10 mm high. The specimens were cured in glass tubes treated with a release agent and were cut using a low-speed diamond saw to produce perfectly parallel end surfaces, which was critical to ensure good compression test results. The parallel end surfaces were in contact with the parallel die surfaces during testing. A screw-driven Instron (Model 4502) was used to conduct the tests. A displacement rate of 0.5 mm min^{-1} was employed.

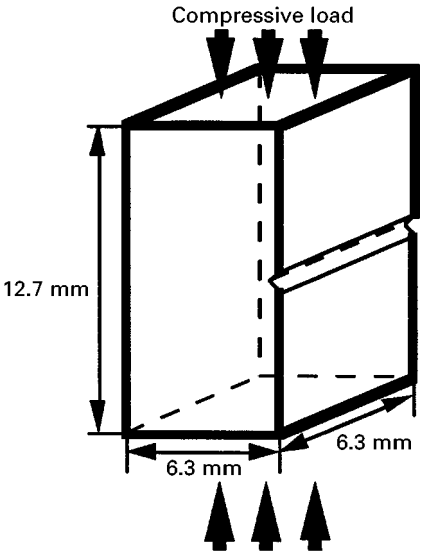

Figure 2 Illustration of a "grooved compression" specimen.

2.4.2. "Grooved compression" test

Rectangular type specimens with a single V-groove on one surface were also utilized for compression tests to generate shear bands. The geometry of the specimen is illustrated in Fig. 2. The dimensions of the rectangular specimens were 12.7 mm high × 6.3 mm wide × 6.3 mm thick. The 0.5 mm deep V-groove was made on one surface of each rectangular specimen. The angle of the V-groove was 42°. Under compression load, shear bands would initiate from the root of the groove and propagate into the specimen. Similar techniques were utilized by Kramer [14] and Wu and Li [15] to investigate the growth of shear bands in polystyrene. A screw-driven Instron (Model 4502) was used to conduct the tests. A displacement rate of 0.5 mm min^{-1} was employed.

2.5. Microscopy

Several microscopy techniques were utilized to determine the deformation and fracture mechanisms. The process zones around "critically" and "sub-critically" loaded cracks in the double-notched four-point bending (DN-4PB) specimens were examined using an optical microscope (OM). The DN-4PB technique is explained in detail by Sue [16]. In this procedure, two nearly identical cracks are made on the same edge of a rectangular specimen. When the sample is loaded in the four-point bend configuration until one of the cracks has failed, the zone in front of the surviving crack possesses characteristics of the deformation behaviour just before the failure. The "critical" crack is the one which fractured and the "sub-critical" crack is the one which survived. Polished petrographic thin (100 μm thick) sections which include the process zone in front of the sub-critical crack tip were prepared

from the mid-plane of the tested specimens. The process zones were observed using a "Nikon Optiphot" optical microscope, in the transmitted light mode, under both bright-field and cross-polarized light. The "grooved" compression specimens were also examined by the petrographic thin section technique under cross-polarized sodium mono-chromatic light. The fracture surfaces of the SEN-3PB specimens were observed using a scanning electron microscope (SEM) "Hitachi S-800".

2.6. Glass transition temperature, T_g, measurement

Glass transition temperatures of resins were determined using differential scanning calorimetry (DSC). A Perkin–Elmer model IIA DSC was used. Measurements were performed at a scanning rate of $10\,^{\circ}C\,min^{-1}$. Mid-point T_g values are reported.

2.7. Small-angle X-ray scattering (SAXS)

SAXS measurements were performed using a Kratky-type camera (Anton Paar, Austria) in CuK_α radiation to detect possible microphase separation. The diffracted radiation was registered by a position-sensitive proportional counter (M-Broun, Germany, model OED 50) in the 2θ interval ranging from 0.04°–0.06° up to 6.6° simultaneously (the minimum accessible angle depends on the geometry and the scattering power of the samples). This angular interval corresponds to a reciprocal space interval ranging from $k_{min} = 0.03\,nm^{-1}$ to $k_{max} = 4.7\,nm^{-1}$, where $k = 4\pi\sin\theta/\lambda$ is the usual diffraction vector, θ is the diffraction angle and λ is the wavelength of the radiation (0.154 nm). It can be estimated that the maximum particle-size resolution of the instrument is in the range $\sim$200 nm. The SAXS curves from independently scattering particles can be analysed with the Guinier approximation [17]

$$I(k) \sim \exp(-k^2Rg^2/3) \quad (4)$$

where $I(k)$ is the diffracted intensity and Rg is the radius of gyration. For spherical particles, the geometrical radius is given by $R = [(5/3)\,Rg]^{1/2}$.

3. Results and discussion

3.1. Cross-link density

The molecular weight between cross-links, M_{nc}, of all epoxy networks used in this study was thought to be the same, because DER332 was cured with the same stoichiometric amount of DDS and the same curing condition in every case. However, in order to ascertain that the M_{nc} is identical among these cured resins, which include different amounts of PES, the following empirical relationship between M_{nc} and T_g of the resin, suggested by Nielsen [18], was used

$$T_g - T_{go} = 3.9 \times 10^4 M_{nc}^{-1} \quad (5)$$

where T_{go} is the glass transition temperature of the corresponding linear polymer. Bellenger *et al.* [19] have quoted 364 K as the value of T_{go} for DGEBA/DDS materials. Although this method of determining M_{nc} may not have a high degree of accuracy, it is considered to be sufficient for comparing the M_{nc} of the various epoxy/PES blends. The estimated cross-link density for the non-modified and PES-modified epoxies are shown in Table I. The T_g of pure epoxy and PES was 194 and 255 °C, respectively. In the case of PES-modified epoxies (PES content; 10–30 wt %), a single T_g was detected at an almost identical temperature (193–196 °C) for all the systems, irrespective of the PES concentration. These results apparently indicate that the PES modification has practically no effect on the T_g and the corresponding cross-link density of the epoxy resin, at least in the range discussed in this paper.

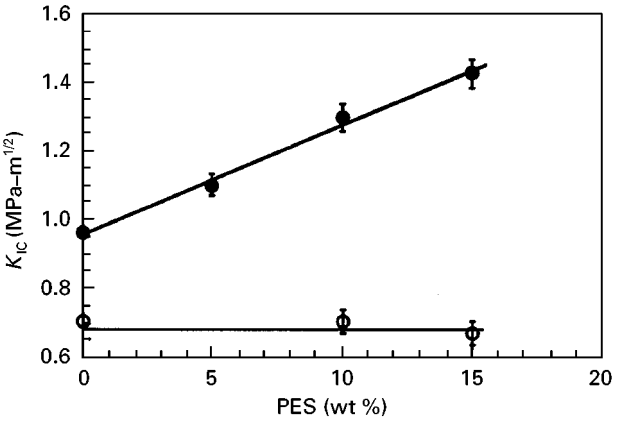

Figure 3 Fracture toughness of cured epoxies versus PES concentration. (○) Fracture toughness of the DDS-cured epoxy is not increased by simply adding PES. However, in the presence of rubber particles as a third component (●), the fracture toughness increases with increasing PES concentration.

TABLE I T_g and molecular weight between cross-links

Formulation	T_g (°C)	M_{nc} (g mol^{-1})
DER332/DDS (pure epoxy)	194	379
DER332/DDS/PES (10%)	196	371
DER332/DDS/PES (20%)	193	382
DER332/DDS/PES (30%)	193	382

3.2. Fracture toughness measurement

The relationships between fracture toughness, K_{IC}, and the PES concentration (wt %) of various DDS-cured DGEBA/PES systems (binary blends) and DDS-cured DGEBA/PES/rubber systems (ternary blends) are shown in Fig. 3. K_{IC} values of all PES-modified epoxy resins without rubber were found to be around 0.7 MPa–m$^{1/2}$. Therefore, the fracture toughness of the DDS-cured epoxy was not enhanced by simply adding PES. On the other hand, K_{IC} values of the PES-modified epoxy resins with 10 wt % rubber increased with increasing PES concentration. For example, the K_{IC} value of the 15 wt % PES-modified epoxy with 10 wt % rubber reached 1.4 MPa–m$^{1/2}$. Therefore, it appears that the toughenability of the DDS-cured epoxy is enhanced by incorporating PES.

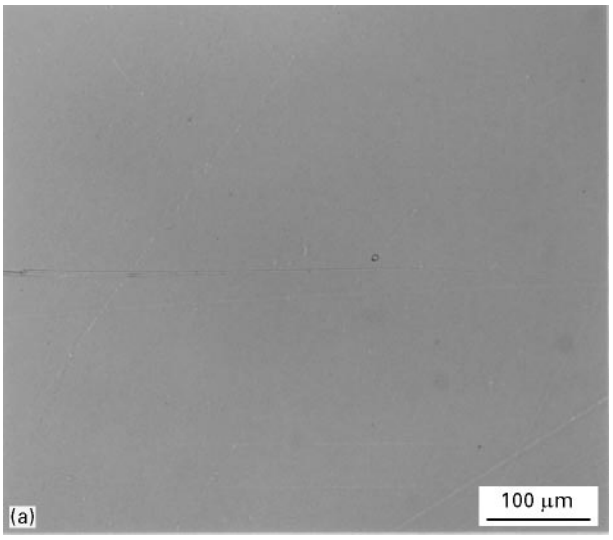

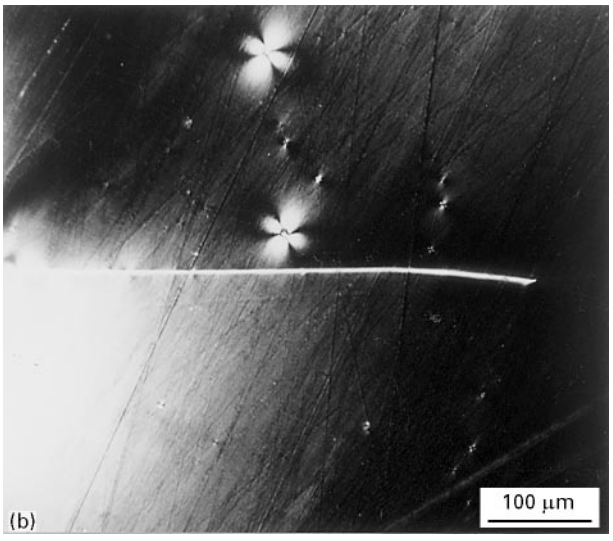

Figure 4 Optical micrograph of a thin section taken mid-plane and near the crack tip of a DN-4PB sample of DER332/DDS (unmodified epoxy), viewed (a) in bright-field and (b) cross-polarized light. Note the absence of a damage zone.

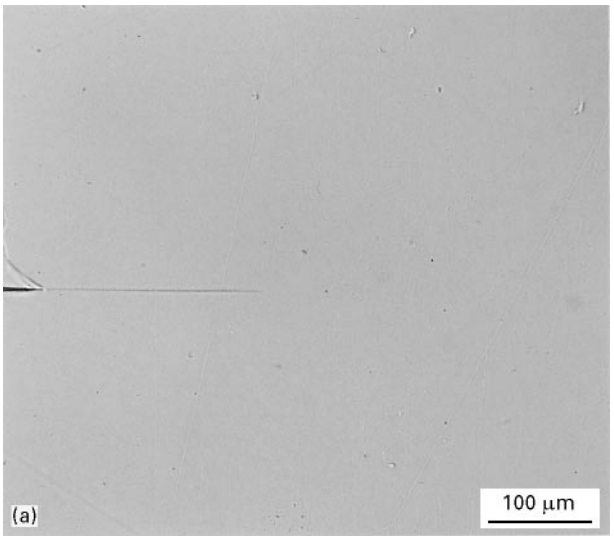

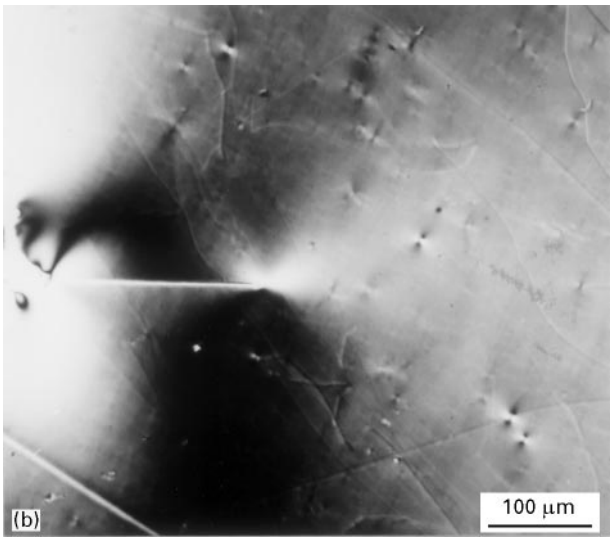

Figure 5 Optical micrograph of a thin section taken mid-plane and near the crack tip of a DN-4PB sample of DER332/DDS/PES (15%), viewed in (a) bright-field and (b) cross-polarized light. Note the absence of a damage zone.

It should be noted that this trend of PES-modification is similar to the effect of reducing cross-link density on toughenability as described by Pearson and Yee [2].

3.3. Toughening mechanisms

Figs 4–7, respectively, show the process zone in front of the surviving "sub-critical" crack in the unmodified epoxy, 15 wt % PES-modified epoxy, 10 wt % rubber-modified epoxy, and 15 wt % PES–10 wt % rubber-modified epoxy blends. The micrographs were taken under both bright-field and cross-polarized light. Figs 4 and 5 show that almost no deformation zone or birefringence was observed in front of the crack tip of the unmodified epoxy and the PES-modified epoxy. This means that no noticeable plastic deformation occurred in these systems, which is consistent with the observation of no increase in toughness of the resins with only PES-modification.

On the other hand, in the case of rubber-modified epoxy and PES-rubber-modified epoxy (Figs 6 and 7), two distinct regions were observed in front of the crack tip. One region is a large circular zone that radiates out around the crack tip. Another region is a smaller, darker elliptical zone that lies inside the circular zone. This type of crack-tip deformation zone has also been reported, by Parker *et al.* [20], in a rubber-toughened polycarbonate. As described by these authors, the contrast in intensity is due to the differences in the concentration and the extent of cavitation of the rubber-particles, as well as the amount of shear deformation within the two zones. The outer circular zone supposedly contains cavitated rubber particles. No birefringence is observed in this zone, which indicates that there is no plastic deformation. In the inner elliptical region, birefringence should be noticed under cross-polarized light, which indicates that plastic deformation occurs in this zone.

In the case of rubber-modified epoxy without PES modification (Fig. 6), small-scale plastic deformation was observed, which explains the small increase in toughness. This is consistent with reports by other researchers that even highly cross-linked epoxy can undergo small-scale shear yielding and be toughened

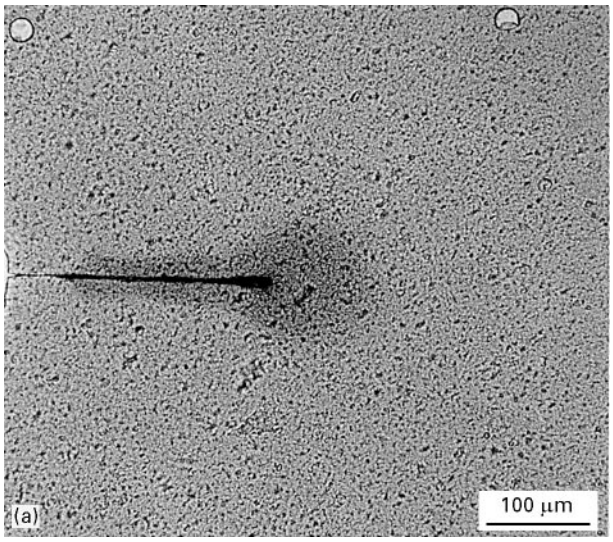

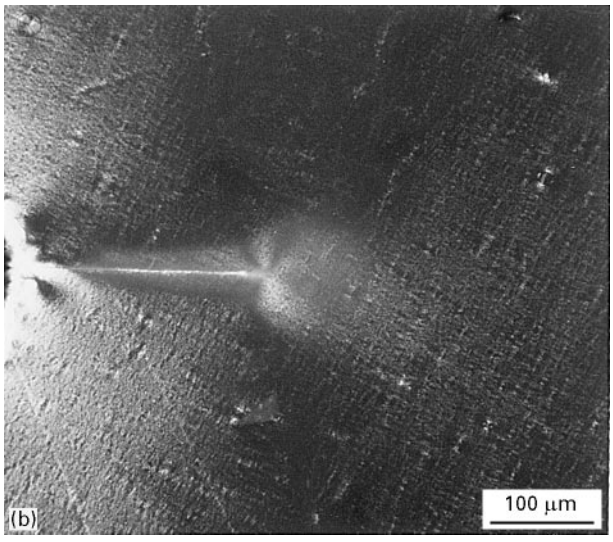

Figure 6 Optical micrograph of a thin section taken mid-plane and near the crack tip of a DN-4PB sample of DER332/DDS/EXL-2611 (10%), viewed in (a) bright-field and (b) cross-polarized light. Note the presence of a circular zone and a darker elliptical zone (a). The elliptical zone is birefringent, indicating that the matrix has shear yielded in this zone (b).

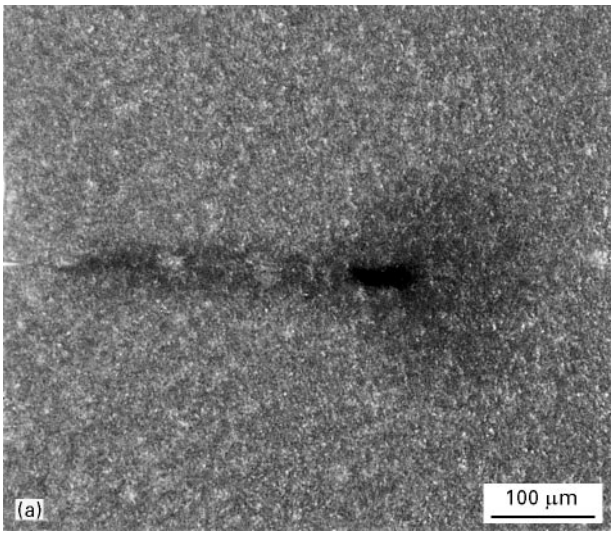

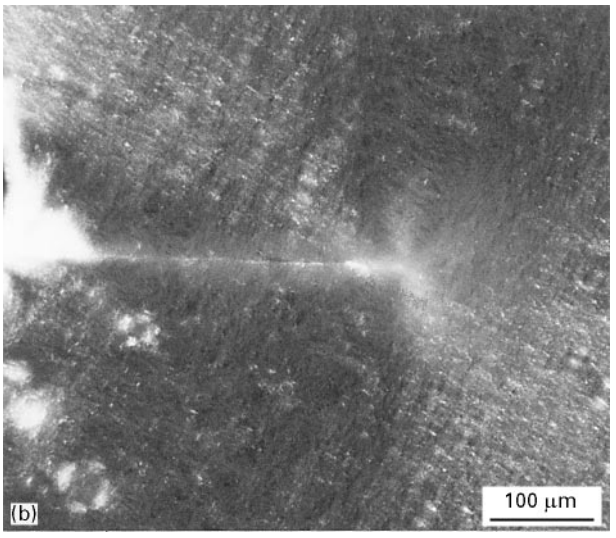

Figure 7 Optical micrograph of a thin section taken mid-plane and near the crack tip of a DN-4PB sample of DER332/DDS/PES (15%)/EXL-2611 (10%), viewed in (a) bright-field and (b) cross-polarized light. Note the larger size of the circular zone and the darker elliptical zone than that of Fig. 6. The more birefringence from the elliptical zone indicates that more plastic deformation has occurred.

to some extent when sub-micrometre-size core–shell rubber particles are added [16, 21]. On the other hand, in the case of the PES-rubber-modified ternary blend (Fig. 7), it is noted that the size of the deformation zone was much larger than that of the epoxy–rubber binary blend. The larger size of the elliptical zone and the stronger birefringence indicate that more extensive plastic deformation occurred in this system, which is consistent with the significant increase in toughness as shown in Fig. 3. Figs 8 and 9 show the areas beneath the wake of the "critical" crack of the rubber-modified epoxy (binary blend) and the PES-rubber-modified epoxy (ternary blend), respectively. The birefringence from the deformation zone of the ternary blend is much stronger than that of the binary blend, again indicating that more plastic deformation occurred in the ternary blend than in the binary counterpart.

Fracture surfaces of the ternary blends with 0, 5, 10 and 15 wt % PES are shown in Figs 10–13, respectively. All of these resins include 10 wt % rubber particles. The crack tip process zone region is observed in these micrographs. Almost all particles are found to cavitate in the process zone, irrespective of the PES amount. It should be noted, however, that a larger distortion of the holes is observed in the blend with 15% PES than in the blend without PES, which indicates that more shear-yielding deformation of the matrix resin surrounding the cavities occurs in the PES-modified epoxy than in the resin without PES.

All this microscopic evidence appears to substantiate the claim that the toughenability of the DDS-cured epoxy has been enhanced by the incorporation of PES. However, unfortunately, the particle dispersion was not consistent throughout these blends. Efforts to achieve uniform rubber particle dispersion had not been very successful. This uncontrolled factor on the particle dispersion might influence the toughness and the toughening mechanism [22]. Therefore, to eliminate the uncontrolled dispersion factor, the

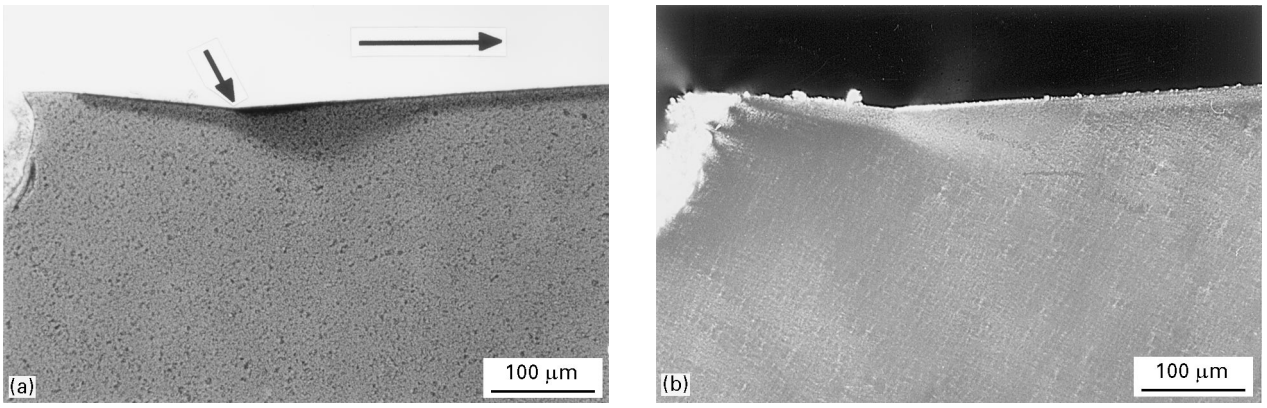

Figure 8 Optical micrograph, viewed in (a) bright-field and (b) cross-polarized light, of the region below the fracture surface of DER332/DDS/EXL-2611 (10%). The small arrow indicates the original crack tip position. The large arrow indicates the crack propagation direction.

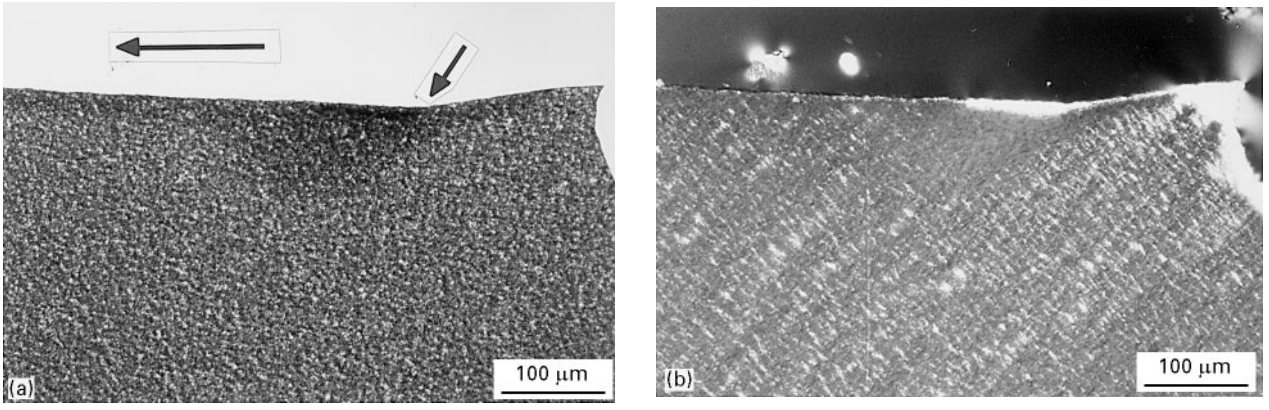

Figure 9 Optical micrograph, viewed in (a) bright field and (b) cross-polarized light, of the region below the fracture surface of DER332/DDS/PES (15%)/EXL-2611 (10%). Note that the birefringence from the deformation zone of this ternary blend is stronger than that of binary blend in Fig. 8. The small arrow indicates the original crack tip position. The large arrow indicates the crack propagation direction.

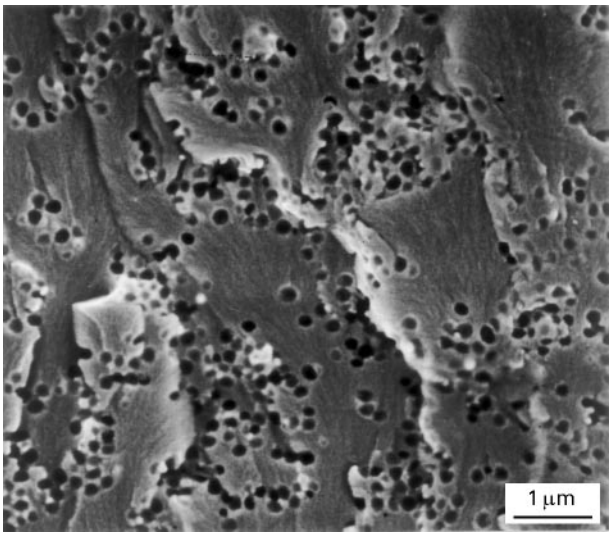

Figure 10 Scanning electron micrograph of the fracture surface of a SEN-3PB specimen of DER332/DDS/EXL-2611 (10%), taken near the crack-arrest region (stress-whitened zone).

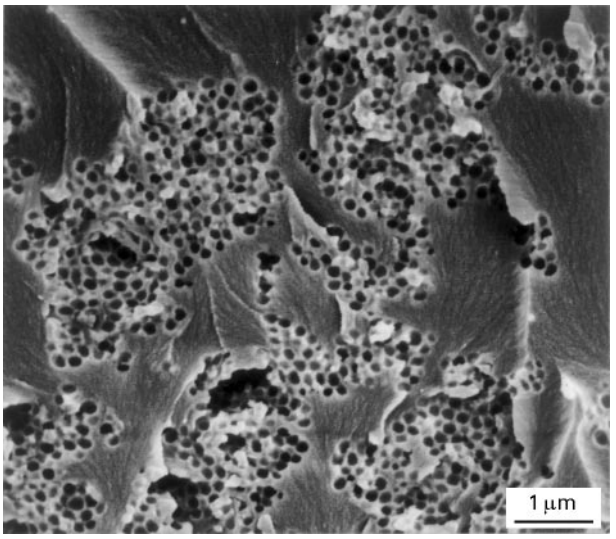

Figure 11 Scanning electron micrograph of the fracture surface of a SEN-3PB specimen of DER332/DDS/PES (5%)/EXL-2611 (10%), taken near the crack-arrest region (stress-whitened zone).

ductility of a series of PES-modified epoxy without rubber particles was examined.

It should be pointed out here that no signs of phase separation were observed from the scanning electron micrographs of the fracture surfaces, either in the PES-rich phase or the epoxy-rich phase. More discussion will be given in a later section on this issue based on SAXS studies.

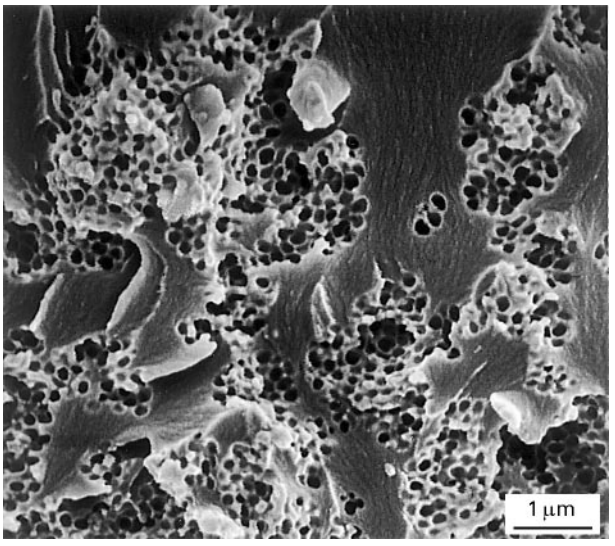

Figure 12 Scanning electron micrograph of the fracture surface of a SEN-3PB specimen of DER332/DDS/PES (10%)/EXL-2611 (10%), taken near the crack-arrest region (stress-whitened zone).

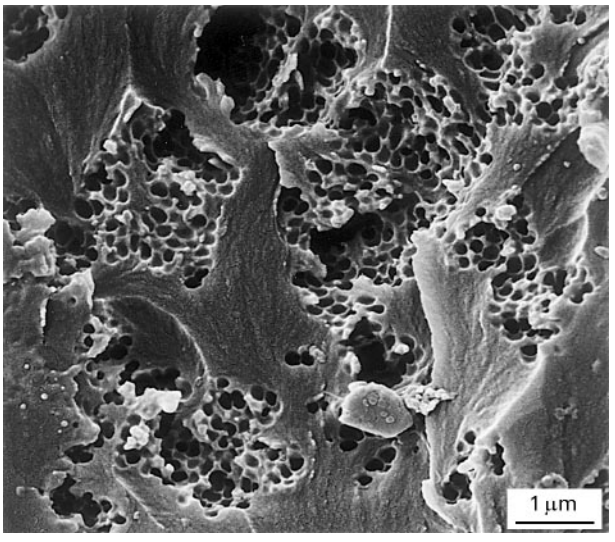

Figure 13 Scanning electron micrograph of the fracture surface of a SEN-3PB specimen of DER332/DDS/PES (15%)/EXL-2611 (10%), taken near the crack-arrest region (stress-whitened zone).

3.4. Shear ductility of the epoxy/PES blends without rubber particles

3.4.1. Uniaxial compression test

If the concept that the toughenability of a resin is mainly dominated by its ductility [2] is correct, then more toughenable resins should exhibit more ductile behaviour under uniaxial compression. So, if PES-modification has any effect on the toughenability of the DDS-cured epoxy resin, a change in ductility should be detected.

The ductility of a material can be determined from the stress–strain behaviour under uniaxial compression. Representative stress–strain behaviours of unmodified epoxy and PES-modified epoxies are shown in Fig. 14. The relationships between yield stress, final breaking strength, final breaking strain and the amount of PES are shown in Fig. 15. It can be seen that even

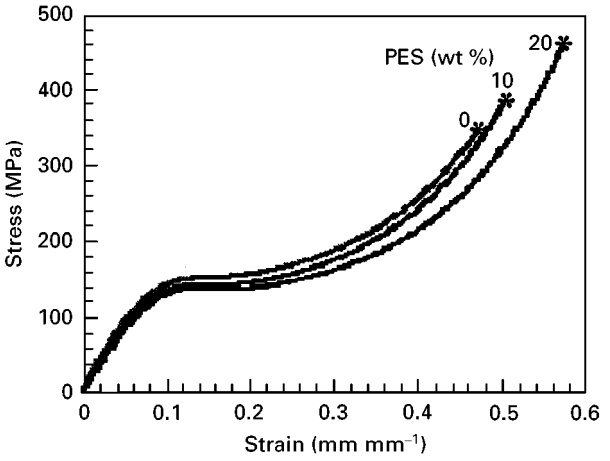

Figure 14 Uniaxial compression test results of an unmodified epoxy and PES-modified epoxies. Note that the yield stress decreases and the final strain at failure increases with increasing PES concentration. Temperature = 23 °C, strain rate = 8.3×10^{-4} s^{-1}.

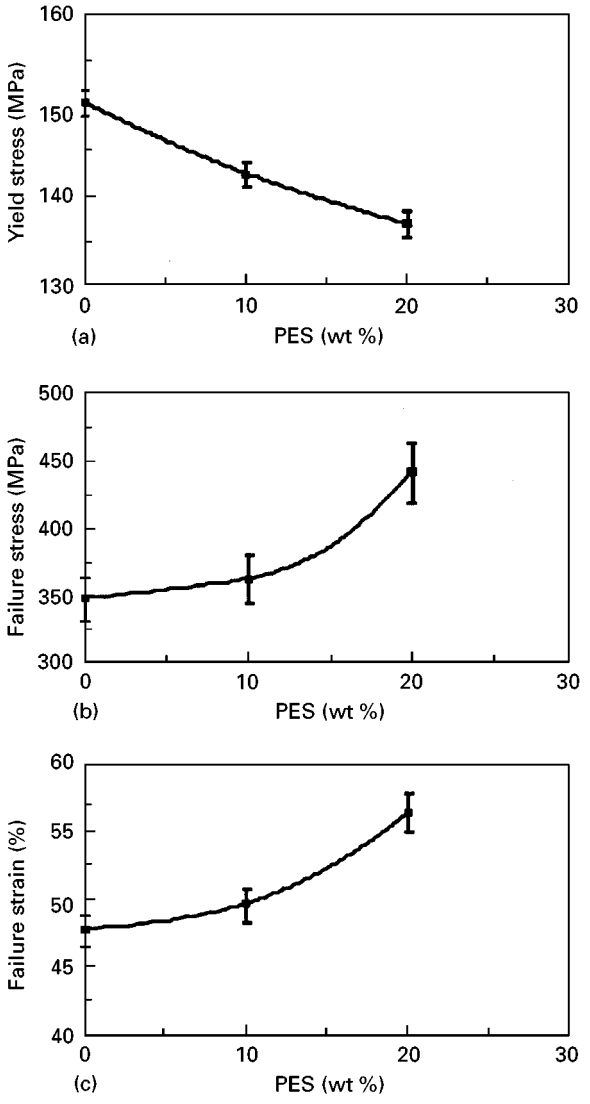

Figure 15 (a) Yield stress, (b) final failure strength and (c) final failure strain in uniaxial compression tests versus the PES concentration. Temperature = 23 °C, strain rate = 8.3×10^{-4} s^{-1}.

DDS-cured highly cross-linked epoxy can yield and have a relatively large failure strain under a uniaxial compressive load. The final fracture seems to occur in the shear mode, which can be determined from

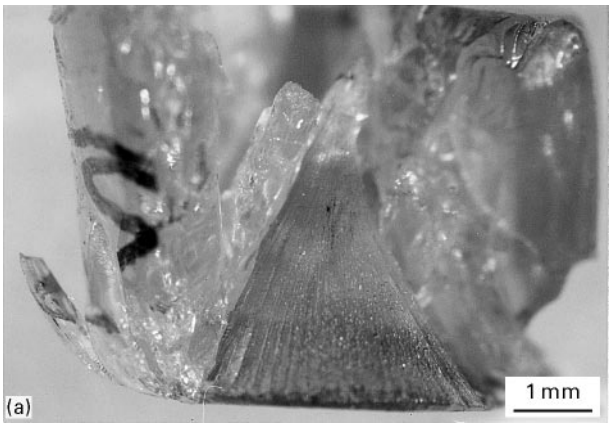

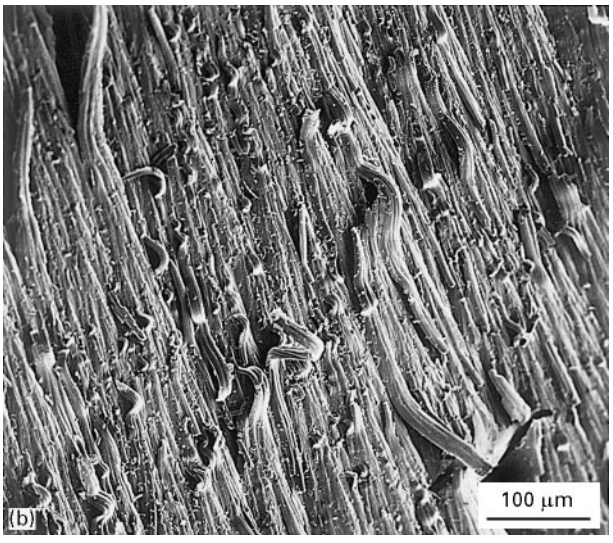

Figure 16 (a) Fracture fragments taken after the uniaxial compression test. Note the cup–cone type fragment, indicating that the final fracture occurred in shear mode. (b) Scanning electron micrograph of the fracture surface of the cup–cone type fragment shown in (a). Note the flow lines, indicating shear yield and cold draw.

the characteristic flow lines observed on the cup–cone type fracture surfaces, as shown in Fig. 16. This suggests that the compression test can serve to quantify the "shear ductility". From Fig. 14, it can be seen that the yield stress of PES-modified resin decreases and the final breaking strain of the resin increases with increasing PES concentration. Also, strain softening occurs in the 20 wt % PES-modified epoxy resin. The stress–strain behaviours indicate that the intrinsic ductility of DDS-cured epoxy has been enhanced by incorporating PES. The increased ductility is thought to be the source of the higher toughenability of the PES-modified epoxy relative to the unmodified epoxy resin.

3.4.2. "Grooved compression" test

The "grooved compression" test was also utilized to further assess the effect of PES-modification on the shear ductility of the DDS-cured epoxy resin. When the uniaxial compression load was applied to a specimen with a shallow groove, two shear deformation bands were formed from the root of the groove. The extent of plastic deformation in the shear bands is an indication of the amount of energy absorbed. So, the

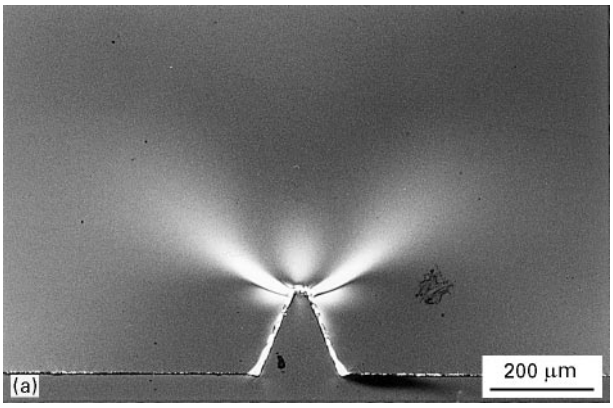

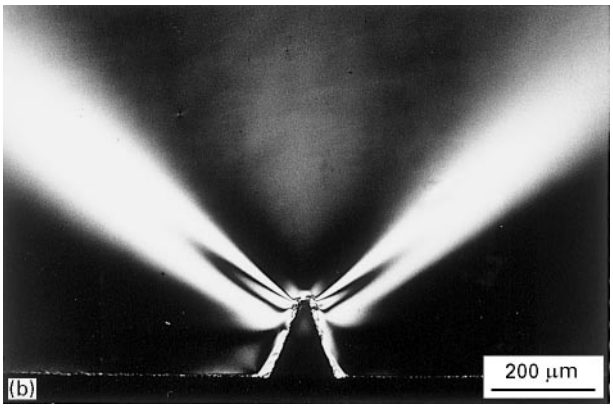

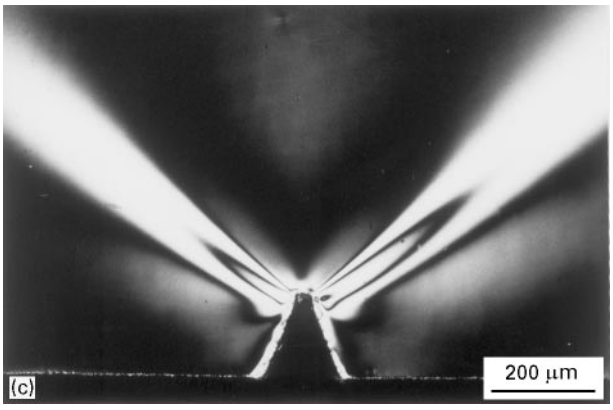

Figure 17 Optical micrograph, taken under cross-polarized sodium light, of a thin section from the mid-plane of a grooved compression sample. The given average stress was 135 MPa. (a) DER332/DDS (unmodified epoxy), (b) DER332/DDS/PES (10%), (c) DER332/DDS/PES (20%).

difference in the extent of shear deformation then reflects the difference of the resin ductility. Optical micrographs of the shear bands of unmodified epoxies, 10 wt % PES-modified epoxies and 20 wt % PES-modified epoxies, under a given overall stress (135 MPa) or a given overall strain (15%), are compared in Figs 17 and 18. Large shear bands were observed in the form of the dark and light bands: fringes, under cross-polarized sodium mono-chromatic light. The size of the shear bands and the corresponding birefringent band became longer and wider with increasing PES addition in both the same average stress and the same average strain cases. One interesting feature observed is the existence of strain distribution within a shear band. Each fringe indicates

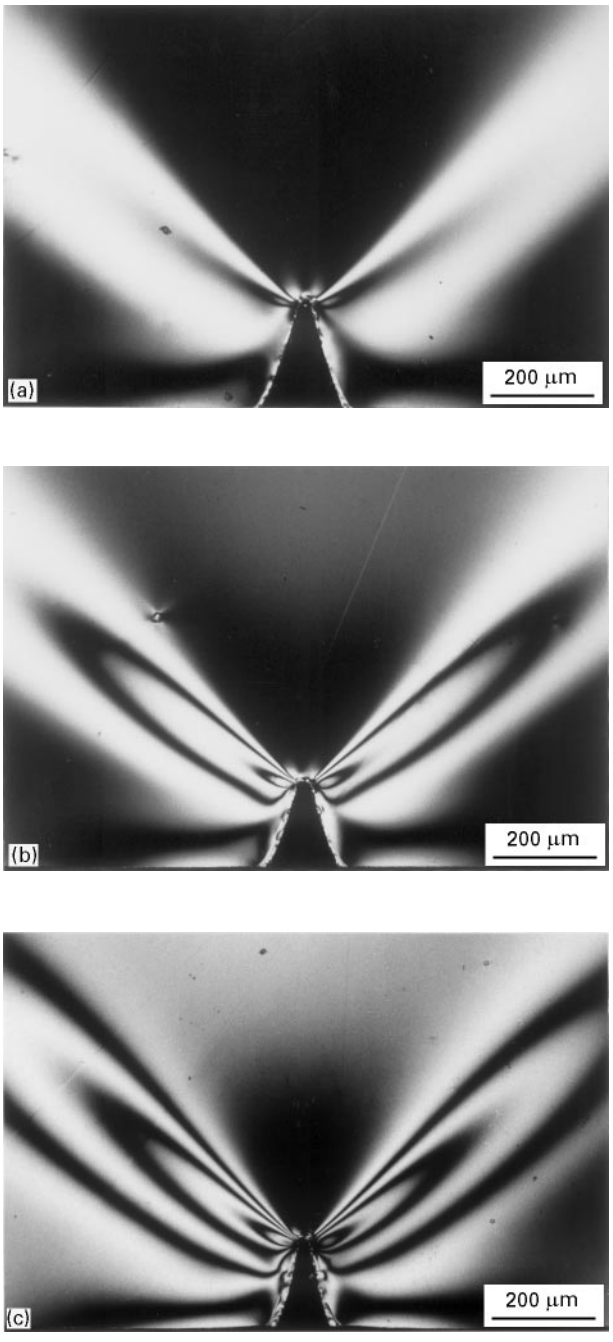

Figure 18 Optical micrograph, taken under cross-polarized sodium light, of a thin section from mid-plane of a grooved compression sample. The given average strain was 15% (a) DER332/DDS (unmodified epoxy), (b) DER332/DDS/PES (10%), (c) DER332/DDS/PES (20%).

a different strain level. The region closer to the root of the groove seems to experience a higher strain and sharp gradient. The number of fringes in the shear bands was observed to increase with the PES concentration. These results indicate a high concentration of plastic strain. They also indicate that the intrinsic ductility (shear deformation ability) of the highly cross-linked epoxy has been enhanced by incorporating PES. We did not attempt to determine the plastic strain in these shear bands from the birefringence because a strain–birefringence calibration was not possible owing to the narrowness of the shear bands.

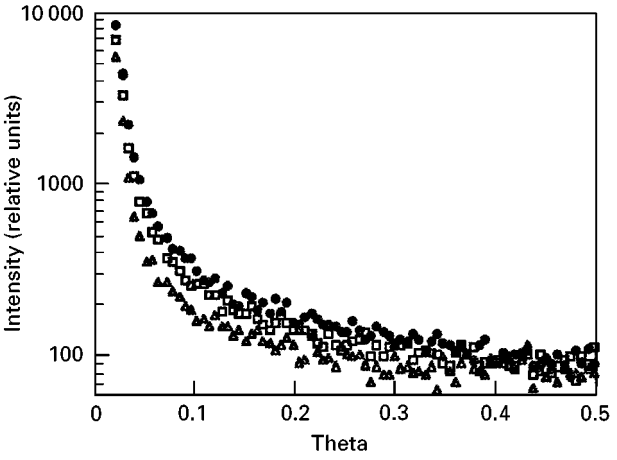

Figure 19 SAXS intensity scans of (△) pure epoxy, (□) 10% PES-modified epoxy and (●) 20% PES-modified epoxy.

3.5. Phase separation of PES-modified epoxy

With the enhancement in ductility demonstrated, we then attempted to probe the elements responsible for the enhancement. First, the microstructure of the PES-modified epoxy was considered. As mentioned above, no clear evidence of phase separation was observed from SEM on the fracture surfaces of the PES-modified epoxies. In addition, all cured resin plaques were visually transparent. However, the possibility of micro-phase separation under 400 nm scale, the lower limit of visible light, still exists.

Therefore, SAXS measurements were performed to examine whether micro-phase separation occurred in the PES-modified epoxy. The SAXS intensity scans of unmodified epoxy, 10% PES-modified epoxy and 20% PES-modified epoxy are shown in Fig. 19. The results indicate clearly that phase separation (the difference in electron density) exists in the PES-modified epoxies. A consistent interpretation of these results is microsegregation of PES-rich phase into the epoxy network. As mentioned in Section 2.7, the Guinier approximation for calculating the particle size of different phases can be used only in the case of independent scattering. Therefore, the Guinier approximation was applied only to the case of the 10% PES-modified epoxy. Assuming that the particles are spherical, the average radius of the micro-phase was then deduced to be 36.2 nm.

So, one possible explanation for the ductility enhancement is that, because the epoxy network does not have complete miscibility with the PES, the molecular conformation of the epoxy network might have been changed in the nano-scale phase separation process. This change in nano-scale structure may have increased the mobility of the network. It is interesting to note that the T_g of these nanometre-size domains are not detectable by DSC. It is quite possible that the phase boundary is not very discrete.

4. Conclusion

In rubber-toughening of epoxies, the intrinsic ability of the matrix resin to shear-deform, in other words,

the "ductility" of the matrix resin, is considered a fundamental requirement for a material to be toughenable by the incorporation of a dispersed rubber phase [2]. In this work, it was found that the shear ductility of the DDS-cured epoxy could be enhanced without reducing the T_g and cross-linking density by the incorporation of PES. Also, the yield stress of the highly cross-linked epoxy was found to decrease; the strain softening behaviour became more pronounced, and the final breaking strain was increased. Moreover, in the grooved compression tests, the extent of shear bands was observed to increase with the PES addition, indicating that PES-modified epoxy is more capable of storing plastic energy. The fracture toughness of DDS-cured epoxy was not enhanced by simply adding PES, indicating that the PES addition is not sufficient to improve the deformation ability under a highly triaxial tensile stress state as in front of a crack tip. However, in the presence of rubber particles as a third component, toughness of the PES-rubber-modified epoxy was observed to increase with the PES concentration. The toughening mechanisms were identical to those reported previously for other modified blends [2, 4, 5], which are rubber cavitation and subsequent plastic deformation of the matrix resin. These results imply that the intrinsic ductility, which had been enhanced by the PES addition, was only activated under the stress-state change due to the cavitation of the rubber particles. The availability of increasing matrix ductility seems to be responsible for the increase in toughness. Therefore, it is concluded that the incorporation of a suitable ductile thermoplastic resin is one way to enhance the intrinsic shear ductility and toughenability of highly cross-linked resins.

Acknowledgement

This work was financially supported by Toray Industries, Inc. We thank Dr Hristo A. Hristov and Mr Christopher L. Soles, University of Michigan, for their help in performing the SAXS experiments.

References

1. R. J. YOUNG and P. A. LOVELL, "Introduction to Polymers", 2nd Edn (Chapman and Hall, London, 1991) pp. 4, 379–80.
2. R. A. PEARSON and A. F. YEE, *J. Mater. Sci.* **24** (1989) 2571.
3. A. J. KINLOCH, C. A. FINCH and S. HASHEMI, *Polym. Commun.* **28** (1987) 322.
4. A. F. YEE and R. A. PEARSON, *J. Mater. Sci.* **21** (1986) 2462.
5. R. A. PEARSON and A. F. YEE, *ibid.* **21** (1986) 2475.
6. H.-J. SUE, PhD Thesis, The University of Michigan, Ann Arbor, MI (1988).
7. G. B. PORTELLI, W. J. SCHULTZ, R. C. JORDAN and S. C. HACKETT, in "Proceedings of the 20th International SAMPE Technical Conference", edited by H. L. Chess, S. P. Prosen, J. W. Davis and J. A. Heth, Minneapolis, September (SAMPE, 1988) Vol. 20, p. 20.
8. R. S. BAUER, L. M. SCHLAUDT and C. A. BLACKBARN, in "Proceedings of the 34th International SAMPE Symposium", edited by G. A. Zakrzewski, D. Mazenko, S. T. Peters and C. D. Dean, Reno, May (SAMPE, 1989) Vol. 34, p. 917.
9. C. B. BUCKNALL, I. K. PARTRIDGE, L. JAYLE, I. NOZUE, A. FERNYHOUGH and J. N. HAY, *Polym. Prepr.* **33** (1972) 378.
10. C. B. BUCKNALL, C. M. GOMEZ and I. QUINTARD, *Polymer* **35** (1994) 353.
11. ASTM D5045-91 (American Society for Testing and Materials, Philadelphia, PA, 1991).
12. W. F. BROWN Jr and J. E. SRAWLEY, "Plane strain crack toughness testing of high strength metallic materials", ASTM STP 410 (American Society for Testing and Materials, Philadelphia, PA, 1966) p. 13.
13. ASTM D695-90 (American Society for Testing and Materials Philadelphia, PA, 1990).
14. E. J. KRAMER, *J. Polym. Sci. Polym. Phys. Ed.* **13** (1975) 509.
15. J. B. C. WU and J. C. M. LI, *J. Mater. Sci.* **11** (1976) 434.
16. H.-J. SUE, *Polym. Eng. Sci.* **31** (1991) 288.
17. G. POROD, in "Small Angle X-ray Scattering", edited by O. Glatter and O. Kratky (Academic Press, New York, 1982) p.17.
18. L. E. NIELSEN, *J. Macromol. Sci. Rev. Macromol. Chem.* **C3** (1969) 77.
19. V. BELLENGER, J. VERDU and E. MOREL, *J. Polym. Sci.* **B25** (1987) 1219.
20. D. S. PARKER, H.-J. SUE, J. HUANG and A. F. YEE, *Polymer* **31** (1990) 2267.
21. R. A. PEARSON and A. F. YEE, *J. Mater. Sci.* **26** (1991) 3828.
22. J. HUANG, Y. B. SHI and A. F. YEE, *ACS Polym. Mater. Sci. Eng.* **70** (1994) 258.

Received 1 May 1995
and accepted 13 February 1996